Fundamental Research 1 (2021) 43–49

Contents lists available at ScienceDirect

Fundamental Research

journal homepage: http://www.keaipublishing.com/en/journals/fundamental-research/

Review

Generation of non-classical states of light and their application in deterministic quantum teleportation

Zhi-Hui Yan[a,b], Ji-Liang Qin[a,b], Zhong-Zhong Qin[a,b], Xiao-Long Su[a,b], Xiao-Jun Jia[a,b,*], Chang-De Xie[a,b], Kun-Chi Peng[a,b]

[a] State Key Laboratory of Quantum Optics and Quantum Optics Devices, Institute of Opto-Electronics, Shanxi University, Taiyuan 030006, People's Republic of China
[b] Collaborative Innovation Center of Extreme Optics, Shanxi University, Taiyuan 030006, People's Republic of China

ARTICLE INFO

Keywords:
Quantum optics
Non-Classical states of light
Optical parametric amplifier
Quantum teleportation

ABSTRACT

Non-classical states of light, which include squeezed and entangled states of light, are the cornerstone of quantum mechanics and quantum information sciences. To date, non-classical states of light with much higher quality than before are required to develop high-fidelity quantum information processing and high-precision quantum metrology. Squeezed and entangled states with approximately 10 dB noise below the corresponding shot noise limit have been generated using a series of methods, which means that the noise variance reaches a few percent of the vacuum noise. Quantum teleportation, which means transferring an unknown quantum state from a sending station to a distant receiving station supported by entangled states, is the foundation of quantum computation and quantum communication networks. Quantum teleportation in continuous variable regions is unconditional because the entangled states used are always deterministic. The quantum teleportation distance was recently extended to the order of kilometers, which paves the way for constructing a practical quantum information network.

1. Introduction

Non-classical states of light, including squeezed and entangled states of light, are important resources for fundamental studies of quantum mechanics and applied research into quantum information sciences, such as faster quantum computation, more secure quantum communication, and more precise quantum metrology [1–3]. Light is an ideal carrier for quantum information due to its fast transmission speed and weak interactions with the environment. Quantum information based on discrete-variable (DV) single photons, called quantum bits, has rapidly developed, and high-fidelity quantum information research supported by maximally entangled states has been implemented [1]. Differing from studies in DV regions, continuous-variable (CV) optical fields, called quantum modes, are an alternative method of deterministic quantum information processing due to the unconditional generation, manipulation, and detection technologies of optical fields [2,3]. Therefore, generating CV non-classical states of light is important for quantum information science. Parametric amplification processing inside a cavity with a non-linear crystal is one of the most efficient methods of generating non-classical states of light. An optical parametric amplifier (OPA) usually consists of a non-linear crystal and an optical cavity. The non-linear crystal is used to implement the parametric amplification processing and the optical cavity enhances parametric processing to generate high-quality non-classical states. According to the phase-matching condition of the signal and idler beams, OPA can be divided into degenerate optical parametric amplifiers (DOPAs) and non-degenerate optical parametric amplifiers (NOPAs). A DOPA consisting of a type I non-linear crystal usually generates a single-mode squeezed state of light [4–6]. Because the noise variance of one quadrature component can be squeezed below the shot noise limit (SNL), while the other conjugate quadrature component is above the SNL to satisfy the Heisenberg uncertainty principle, squeezed states of light have compelling applications in quantum metrology to improve the measurement sensitivity [7–9], such as continuous force and displacement measurements [10], gravitational-wave detection [11, 12], and biological measurements [13]. Einstein-Podolsky-Rosen (EPR) bipartite-entangled states can be obtained when two squeezed states from two sets of DOPAs interfere on a 50/50 beam splitter [14–16]. Multipartite entanglement is crucial for developing quantum networks [17–21]. If more squeezed states of optical field are generated and coupled on a beam splitter network, the multipartite-entangled state of optical fields can be obtained using Braunstein and Lance's method [2, 17]. NOPA is composed of type II non-linear crystals and optical cavities and produces two polarization-perpendicular optical fields. The coupled mode of output optical fields from NOPA is a two-mode squeezed state,

* Corrresponding author.
E-mail address: jiaxj@sxu.edu.cn (X.-J. Jia).

https://doi.org/10.1016/j.fmre.2020.11.005

Available online 10 December 2020

and if two-mode optical fields are separated by a polarized beam splitter (PBS), they form an EPR bipartite-entangled state [21–24].

With the development of quantum information science, entangled optical fields with a high degree of entanglement are desirable for high-fidelity quantum information processing. One approach to obtain highly entangled states is optimizing the NOPA's condition. Another method to provide high-quality quantum states is quantum manipulation [25–27]. An OPA, which is an ideal phase-sensitive device, can be used to not only generate the non-classical states, but also implement their phase-sensitive manipulation [28–30]. Compared with measurement-based feedback control, coherent feedback control (CFC) manipulates quantum states of light without introducing extra noise [31–35]. The CFC system enables researchers to not only manipulate entangled states to provide the desirable degree of entanglement but also increase the degree of entanglement under the proper conditions [35].

Quantum entanglement can be applied in a variety of quantum information protocols to improve information capability, transmission security, and measurement precision. Quantum teleportation transfers an unknown quantum state from one node to another, which is implemented through the local operation and shared quantum entanglement [36–41]. Quantum teleportation is essential for quantum information science and has been widely applied in many quantum information protocols such as quantum entanglement swapping [42–45], quantum teleportation networks [46], and quantum computation [47–49]. Since quantum teleportation based on bipartite entanglement was proposed and its experimental implementation was based on entangled photon pairs [37], studies on probabilistic quantum teleportation have been widely conducted. Deterministic quantum teleportation of quantum modes based on CV-entangled states has also attracted considerable attention [38–40]. Hybrid quantum teleportation that combines the advantages of DV and CV approaches has been experimentally demonstrated [50,51].

Long-distance quantum teleportation is necessary for practical applications of the global-scale quantum Internet. Breakthroughs have recently been achieved in high-fidelity and long-distance quantum teleportation. Because transmission loss and decoherence are almost negligible in the atmosphere, satellite-based quantum channels offer a promising approach for long-distance quantum teleportation. In 2017, quantum teleportation from the ground to a low-Earth-orbit satellite with a single photon over 1400 km was experimentally demonstrated, which provided a feasible protocol for quantum communication on a global scale [52]. Low-loss optical fibers have also been applied to construct quantum channels for long-distance quantum teleportation [53, 54]. Recently, 6.0 km deterministic teleportation of quantum modes via fiber channels with a fidelity of 0.62 has been achieved [55].

The paper is organized as follows. In Section "Generation of non-classical states of light", the generation of non-classical states of light is investigated and the production of a highly entangled state of light is discussed. In Section "Quantum manipulation of entangled optical fields", the quantum manipulation of entangled states including phase-sensitive manipulation and coherent feedback control of entangled optical fields are introduced. Deterministic quantum teleportation through optical fibers supported by entangled states of light is demonstrated in Section "Fiber channel continuous-variable quantum teleportation". Finally, a brief summary is provided in Section "Conclusion and perspective".

2. Generation of non-classical states of light

The optical EPR-entangled states, called two-mode squeezed states, consist of two sub-modes with quantum correlations between the quadrature amplitude and quadrature phase. If the combination of noise variances of the amplitude sum (difference) and phase difference (sum) of the two sub-modes is smaller than the corresponding SNL, the two sub-modes are inseparable and thus form an optical state with EPR entanglement. Entangled states of light are among the most prominent quantum resources in quantum information science, and over the past few decades, the generation of entangled states has made considerable progress, advancing quantum communication and quantum computation. In 1992, Kimble's group experimentally obtained a pair of CV-entangled optical beams with a NOPA and demonstrated the EPR paradox in the CV system. Since then, the quality of EPR entanglement has been improved by related groups [16, 24, 44].

The inseparability criterion can be used to verify EPR entanglement. In this criterion, the quantum correlation of the Gaussian state is quantified by the correlation variance sum S of the quadrature amplitude and phase [56, 57]:

$$S = \langle \delta^2(\hat{X}_{a1} \pm \hat{X}_{a2})\rangle + \langle \delta^2(\hat{Y}_{a1} \mp \hat{Y}_{a2})\rangle, \tag{1}$$

where a_1 and a_2 are sub-modes of the EPR entanglement, $\hat{X}_{a1(2)}$ and $\hat{Y}_{a1(2)}$ are the operators of amplitude and phase quadratures for each sub-mode, and $\langle \delta^2(\hat{X}_{a1} \pm \hat{X}_{a2})\rangle$ and $\langle \delta^2(\hat{Y}_{a1} \mp \hat{Y}_{a2})\rangle$ are the correlation variances of the quadrature amplitude and phase in two EPR sub-modes. According to the inseparability criterion [56, 57], the sum of the correlation variance between signal and idler optical fields equals 1. If the correlation variance sum is less than the corresponding SNL such that <1, the output fields are CV-entangled states. The strength of the entanglement is measured by the degree of entanglement, which is the ratio between the correlation variance and its corresponding SNL.

It is crucial to generate highly entangled states with a compact quantum device to conduct proof-of-principle experiments for practical applications. To improve the degree of entanglement, our group experimentally demonstrated that quantum correlations of the amplitude and phase quadrature between signal and idler optical fields from a NOPA can be significantly improved using a mode cleaner to reduce phase fluctuations in phase locking systems. Based on these two technical improvements, the entanglement degree of EPR-entangled optical fields enhanced from 4.0 dB to 6.0 dB below the corresponding SNL, that is, $S = 0.25$ [24]. We then designed and constructed an efficient and compact entanglement source, in which a NOPA with triple resonance of the pump, signal, and idler optical fields directly produced highly entangled states by increasing the output coupler's transmissivity. A wedged type-II phase-matching non-linear KTP crystal was used to implement parametric down-conversion of the pump's optical field to generate entangled signals and idler optical fields. Triple resonance was achieved by precisely moving the wedged crystal's position to compensate for dispersion between the pump, signal, and idler optical fields. An EPR-entangled state with amplitude and phase quadrature correlations 8.4 dB below the corresponding SNL was experimentally obtained by this single NOPA [21]. The corresponding correlation variance sum of the amplitude and phase quadrature was $S = 0.14 < 1$.

A NOPA in a deamplification situation (in which the phase difference between the pump field and signal [idler] optical field equals $(2k + 1)\pi$, where k is an integer) outputs an EPR-entangled state with anti-correlation of the quadrature amplitude and correlation of the quadrature phase. By resolving the NOPA's Langevin equation, the correlation variance's dependence on the sub-mode of the EPR entanglement on the NOPA's real parameters can be obtained:

$$S = 1 - \eta \frac{4\sqrt{\frac{P}{P_{th}}}}{\left(1 + \sqrt{\frac{P}{P_{th}}}\right)^2 + 4(2\pi f/\kappa)^2}, \tag{2}$$

where the total efficiency η is the effective NOPA output, which depends on the imperfect detection efficiency of the entanglement measurement system and the NOPA's escape efficiency; f is the sideband's analysis frequency; κ is the NOPA cavity's decay rate; and P and P_{th} are the NOPA's pump power and pump threshold power, respectively. Eq. (2) demonstrates that this is an effective method of obtaining a high degree of entanglement by increasing the transmissivity of the NOPA's output coupler and decreasing the intracavity losses in the signal (idler) optical field.

The experimental setup of the triple-resonance NOPA with a wedged crystal is shown in Fig. 1. A continuous-wave intracavity frequency-

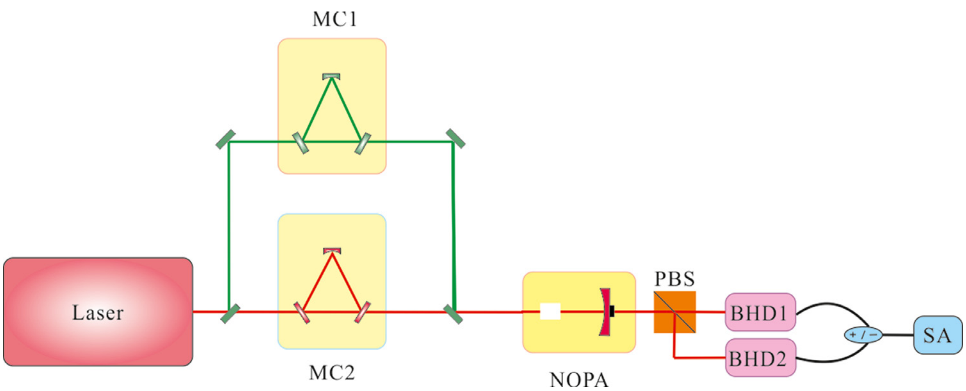

Fig. 1. The experimental setup of the triple-resonance NOPA. MC1-2: Mode cleaner. NOPA: Non-degenerate optical parametric amplifier. PBS: Polarized beam splitter. BHD1-2: Balanced homodyne detector. SA: Spectrum analyzer.

doubling single-frequency Nd:YAP/LBO laser (Yuguang Co.) outputs lasers at 1080 nm and 540 nm. Two ring cavity mode cleaners (MC) are used for spatial-temporal filtering to improve the mode quality and reduce extra amplitude and phase fluctuations at 1080 nm and the pump's optical field at 540 nm, respectively. The output optical fields from the two mode cleaners at 1080 nm and 540 nm are used as the NOPA's seeded signal (idler) and pump optical fields. To avoid the walk-off effect of ordinary and extraordinary optical fields within the crystal, α cut $3*3*10$ mm^3 KTP was used in the experiment as a non-linear crystal with type-II non-critical phase matching [58]. The KTP crystal was placed in a copper oven with a precise temperature controller and moved along the transverse direction for triple resonance. The seeded signal and idler optical fields with horizontal and vertical polarization at 1080 nm resonated in the NOPA by tuning the KTP crystal's temperature to 63 °C. To compensate for dispersion between the pump and signal (idler) optical fields for triple-resonance, a wedged crystal was placed in the optical cavity. When the wedged crystal was transversally moved in the optical cavity, the compensation of the optical paths between different optical fields was complete. The NOPA's cavity length was locked to resonate with the signal's optical field using the Pound–Drever–Hall (PDH) technique. When the NOPA's pump threshold power was 150 mW, two signal and idler optical fields were generated by the intracavity parametric down-conversion process at a pump power of 75 mW.

To measure the entanglement between the signal and idler modes, the amplitude or phase quadrature of the two output modes separated by the PBS were measured using two sets of balanced homodyne detectors (BHDs) consisting of a 50/50 beam splitter and two high-quantum-efficiency photodetectors. When the relative phase between the local and signal (idler) optical fields was locked at 0 or $\pi/2$, two sets of the BHD system's outputs were combined by a positive (negative) power combiner to obtain anti-correlation (correlation) variances between the amplitude or phase quadrature of the signal and idler modes, which were then measured by a spectrum analyzer (SA). The noise powers of the amplitude and phase quadrature measured at 2 MHz showed that the EPR bipartite-entangled state with correlation variances of the amplitude and phase quadrature were 8.4 dB below the corresponding SNL obtained [21].

An efficient method of generating multiple entangled modes was recently proposed utilizing frequency multiplexing in optical parametric processing. Each pair of a DOPA's sideband modes were used for an independent quantum channel for quantum communication because a squeezed field involved a series of EPR-entangled modes at sidebands of $\omega_0 \pm n\omega_{FSR}$, where ω_0 is the half frequency of the DOPA's pump field, n is an integer, and ω_{FSR} is the DOPA's free spectral range. Each pair of sideband modes formed an EPR-entangled state that could be used by an independent quantum channel for quantum communication. By applying an accurate frequency-filtered system, fourfold entangled sideband modes with entanglements of 8.0, 7.9, 7.2, and 7.6 dB were spatially separated and obtained at the DOPA's first four resonances, respectively.

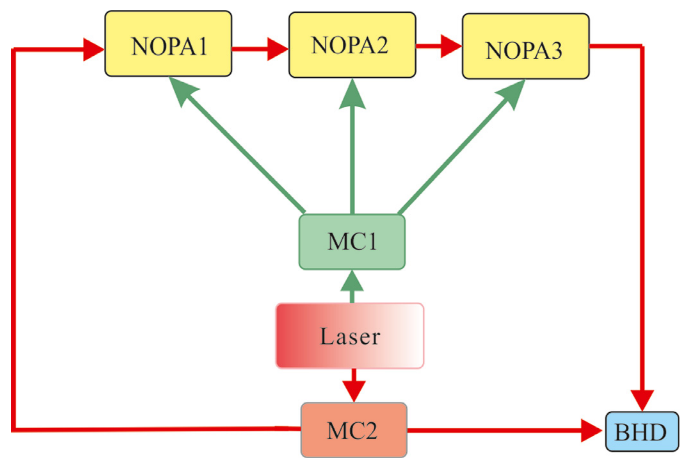

Fig. 2. An experimental schematic of the cascaded entanglement manipulation system. MC1-2: Mode cleaner; NOPA1-3: Nondegenerate optical parametric amplifier; BHD: balanced homodyne detector.

Then four-channel multiplexing quantum dense coding communication with four pairs of extracted entangled sideband modes was experimentally demonstrated by our group [59]. Because these entanglements had wide frequency separation among entangled pairs, the channel capacity of quantum channels significantly increased and cross-talk effect was easily avoided.

3. Quantum manipulation of entangled optical fields

Control is used to find methods of manipulating the evolution of dynamic systems. Control is studied by analyzing dynamic systems in the frequency domain because researchers are mainly interested in its steady-state behavior. Optical parametric processing not only provides desirable quantum states, but also manipulates entangled optical fields for practical applications. Fig. 2 shows an experimental schematic of a cascaded entanglement-manipulation system, which includes a continuous-wave laser, two MCs, and three NOPAs. The output of fundamental and harmonic wave lasers from two mode cleaners is used as the injected signal (idler) optical fields of NOPA1 and the pump optical fields of the three NOPAs, respectively. First, NOPA1 generates an EPR-entangled optical field that is used as the injected optical field of NOPA2 for first-stage quantum manipulation of the entanglement. Then the manipulated EPR optical field from NOPA2 is injected into NOPA3 for second-stage quantum manipulation. The signal and idler optical fields from NOPA3 with orthogonal polarizations are detected by the BHD. The degree of entanglement depends on the status of the three NOPAs. If all three NOPAs are operated simultaneously below the

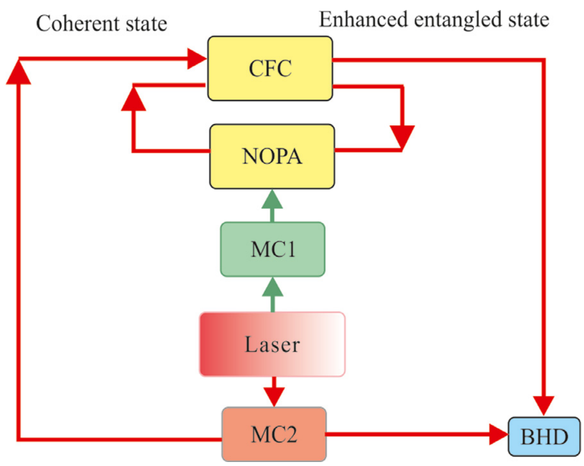

Fig. 3. An experimental schematic of the CFC-NOPA system. MC1-2: Mode cleaner. NOPA: Non-degenerate optical parametric amplifier. CFC: Coherent feedback control. BHD: Balanced homodyne detector.

NOPA's pump threshold power under deamplification conditions, cascaded entanglement enhancement is achieved and the degree of output entanglement improves from −5.3 dB to −8.1 dB [30].

Non-measurement-based coherent feedback control (CFC) is another quantum manipulation method [27]. Compared to measurement-based feedback control, the CFC system introduces no backaction noise into the controlled system and is suitable for manipulating various noise-sensitive quantum states in optical fields. The CFC system can be used to test the principles of linear quantum stochastic control theory [60] for quantum error correction [61]. An experimental schematic of the CFC-NOPA system is shown in Fig. 3. The quantum state is originally produced by a NOPA and then directly injected into the CFC loop. In the CFC loop, non-classical optical fields are split into two parts by a controlled beam splitter: one is fed back to the NOPA and the other is the final output optical field's quantum states. The output optical fields' quantum features can be manipulated by a controlled beam splitter (CBS) because the CFC loop coherently manipulates the NOPA's original output and feeds some of it back into the NOPA to manipulate its performance. The CFC can also be applied in the DOPA system, and squeezing enhancement based on the CFC system was proposed and experimentally realized [62–64]. The CFC system can be extended to multipartite-entangled states of light generated by an OPA. By controlling the transmissivity of a CBS in a CFC loop, the degree of entanglement of output multipartite-entangled optical fields can be significantly improved [34]. The non-measurement-based CFC has been applied to deterministic atomic light entanglement with imperfect retrieval efficiency. Deterministic atomic light entanglement is generated based on the Raman process. It is possible to manipulate atomic light entanglement by tailoring the transmissivity of the CBS of the CFC loop, and the CFC system allows atom-light entanglement enhancement under appropriate conditions [65].

4. Fiber channel continuous-variable quantum teleportation

Due to its extra-low noise characteristics, quantum entanglement has been applied in various quantum information protocols to enhance the procession capabilities, transmission speed, and measurement precision. Quantum teleportation reliably transfers a quantum state from one node to another over long distances by quantum entanglement shared between a sender and distant receiver without any need of the physical traveling of the object. It is essential for quantum entanglement swapping [42–45], quantum teleportation networks [46], and quantum computation [47–49]. Quantum entanglement swapping entangles different particles that have never directly interacted with each other and connects different quantum nodes and quantum networks to produce a quantum repeater [42–45]. Therefore, quantum teleportation is the cornerstone of practical applications of quantum information science.

DV quantum information implements high-fidelity quantum information processing based on post-selected entangled photons and has achieved considerable progress. In 1993, C.H. Bennett et al. proposed a method of teleporting an arbitrary unknown quantum state supported by the classical information channel and quantum correlations [36]. First, two particles with entangled states are generated and distributed to a sender and distant receiver. Then an unknown quantum state to be teleported is jointly measured using one of the entangled particles held by the sender. The measurement results are transmitted to the distant receiver through classical communication channels. The quantum state of the other particle of the entangled state held by the distant receiver is transformed into an unknown input state based on the results of the sender's joint measurement. The unknown input quantum state is destroyed at the sender when it is jointly measured at the sending station and is reconstructed at the receiver when quantum teleportation is complete. In 1997, D. Bouwmeester et al. experimentally completed the first quantum teleportation of quantum bits [37].

Quantum teleportation over long distances is a key building block for constructing a global platform of quantum communication networks. In quantum communication networks, transmission loss and phase noise are inevitable in long-distance transmission channels in practice, and the error probability scales exponentially with the channel length. Optical fibers are widely used in classical communication networks due to their low transmission loss and in quantum information technology to construct large-scale quantum communication networks. In 2003, I. Marcikic et al. accomplished probabilistic quantum teleportation of quantum bits from one laboratory to another connected by a 2.0 km fiber [53]. H. Takesue et al. reported on quantum teleportation over a 100 km optical fiber using four high-detection-efficiency superconducting nanowire single-photon detectors [54]. Satellite-based quantum channels offer a promising alternative approach for quantum teleportation over long distances because photon loss and decoherence are negligible in the atmosphere. Yin et al. and Ma et al. respectively demonstrated quantum teleportation of quantum bits over 100 km free-space quantum channels [66, 67]. A promising method adopts satellite platforms and space links, significantly reducing channel loss because most photon-propagation paths are empty spaces. For quantum communication on a global scale, Ren et al. demonstrated quantum teleportation of independent single-photon quantum bits up to 1400 km from a ground observatory to a low-Earth-orbit satellite [52].

Probabilistic generation and measurement systems make it impossible to instantaneously transfer quantum states [2, 3]. Deterministic quantum teleportation is desirable in quantum communication networks and distributed quantum computation. CV quantum teleportation of quantum modes can enable deterministic quantum teleportation of arbitrary unknown quantum states because the generation, manipulation, and detection of continuous variables are unconditionally complete [38, 40]. Fidelity is used to characterize the performance of quantum state transfers. Using only a classical channel, a fidelity of 1/2 was obtained that was set as the boundary between classical and quantum domains to teleport coherent states. The criterion for evaluating the performance of quantum teleportation of continuous variables has a fidelity value larger than 2/3, which warrants that the teleported state is the best possible remaining copy of the input state [68]. If quantum entanglement is used, the fidelity of quantum teleportation can surpass the boundary of 1/2 and even reach a perfect value of 1.0 with the perfect entanglement [69, 70]. Deterministic quantum teleportation of optical coherent states was first demonstrated with a CV-entangled state of light in 1998 [40].

Transferring non-classical states across quantum communication networks is required for quantum information science. Quantum teleportation of a squeezed state has been demonstrated experimentally. The variance of the teleported squeezed state was smaller than that of the vacuum state input, and the measured fidelity was 0.85, higher than the classical case of 0.73 [71]. Quantum entanglement swapping can be viewed as quantum teleportation of entangled optical fields, enabling us to entangle different particles that never have directly interacted with each other. Two pairs of optical fields with entangled states were produced from two sub-threshold NOPAs and used as quantum channels. Through direct Bell state measurement and feed-forward, one optical beam of an entangled state to be teleported and the other optical beam of the entangled state as a quantum channel that have never directly interacted with each other can be entangled. Quantum correlation degrees of 1.23 and 1.12 dB below the corresponding SNL for the amplitude and phase quadrature were measured, and quantum entanglement swapping transferred the entangled state of optical fields [43]. Hybrid protocols involving DV and CV techniques for quantum information processing are demanding for practical applications because they combine the advantages of both techniques. N. Lee et al. reported experimental quantum teleportation of fragile non-classical wave packets of light using a broadband zero-dispersion teleportation apparatus [50]. Quantum teleportation of photonic quantum bits has been limited by the probabilistic nature of linear optic Bell measurements. S. Takeda et al. experimentally realized deterministic quantum teleportation of quantum bits by adopting a hybrid technique involving CV teleportation of DV quantum bits. CV teleportation was unconditionally completed via optical fields with CV-entangled states. Quantum bits based on a single photon represent a quantum error detection code against photon loss. This experiment allowed reliable quantum bit transfer with imperfect CV-entangled states, and the overall transfer fidelities of four quantum bits were from 0.79 to 0.82, exceeding the teleportation boundary in the no-cloning limit [51].

Deterministic quantum teleportation of various quantum states has achieved considerable progress over short distances. CV quantum teleportation is implemented in laboratories to demonstrate the principle over short distances, limiting the scale of CV quantum information networks. The extension of deterministic quantum teleportation distances is required for practical applications. Because optical fibers are candidates for quantum information channels due to their low transmission loss over long distances, deterministic teleportation over long distances can be realized in fibers. Deterministic quantum teleportation of a coherent state over a fiber channel of 6.0 km was recently experimentally demonstrated by our group [55]. To implement quantum teleportation, it is necessary to generate entangled states of light that match optical fibers' transmission windows, 1.3 μm is an applicable optical fiber transmission window due to its low dispersion. Output optical fields at 1.34 μm and 0.67 μm from a dual wavelength Nd:YVO_4/LBO laser were filtered by two mode cleaners used as the seeded and pump optical fields of a DOPA. The DOPA cavity consisted of a pair of concave mirrors and a 1*2*12 mm^3 PPKTP crystal. The DOPA's length was locked to resonate with the seeded beams via the PDH technique. The phase difference between the pump laser and seeded optical fields was maintained at (2k+1)π (where k is an integer) so the DOPA operated under parametric deamplification conditions to produce non-classical optical fields. When the polarization of the pump and seeded optical fields were in the vertical direction, the DOPA generated a single-mode amplitude quadrature squeezed state of light. The noise power of the amplitude quadrature of the output optical fields was 3.17 dB below the corresponding SNL at a side band of 3 MHz. If the pump optical field's polarization was horizontal, the combined optical field of the signal and idler optical fields with perpendicular polarization was 45° relative to the PPKTP crystal's y axis, and the DOPA operated under type-II quasi phase-matching conditions. The simultaneous resonance of the DOPA's signal and idler beams was realized by tuning the PPKTP crystal's temperature, and the output signal and idler optical fields constituted an EPR-entangled state. The noise powers of the quadrature amplitude sum and quadrature phase difference were 2.27 dB and 2.23 dB below the corresponding SNL, respectively [72].

A schematic diagram of deterministic quantum teleportation through fiber channels is shown in Fig. 4. The coherent state is a minimum uncertainty state, and the uncertainties of its two quadrature components are equal, which is the closest quantum approximation of a laser. Alice and Bob shared an EPR-entangled state optical field distributed by optical fibers. The optical field received by Alice ($\hat{a}_{EPR1}$) and the unknown quantum state ($\hat{a}_{in}$) were combined in a 50/50 beam splitter. The amplitude quadrature $\hat{X}_{tel} = (\hat{X}_{in} + \hat{X}_{EPR1})/\sqrt{2}$ and phase quadrature $\hat{Y}_{tel} = (\hat{Y}_{in} - \hat{Y}_{EPR1})/\sqrt{2}$ of the 50/50 beam splitter's two output fields were measured by two sets of BHDs, respectively. These joint measurements of the input state and optical field EPR1 at Alice were transmitted to Bob via two classical channels. Bob displaced his optical field of the EPR-entangled state ($\hat{a}_{EPR2}$) with an amplitude electro-optic modulator (AM) and a phase electro-optic modulator (PM) according to the received measurement results. The input quantum state destroyed by the joint measurements by Alice was recovered by Bob supported by non-local quantum entanglement. To assess the quantum teleportation, Victor verified the teleportation performance with a BHD. Fidelity $F = \langle\Psi_{in}|\hat{\rho}_{out}|\Psi_{in}\rangle$ is usually used to quantify the performance of quantum teleportation. It represents the overlap between the input state Ψ_{in} and the output state characterized by the density matrix $\hat{\rho}_{out}$ [68]. In the optical fiber channel, the influence of the transmission efficiency and extra noise inside the optical fibers must be considered. The extra noise resulting from optical fiber channels reduces entanglement and the quantum teleportation distance. The extra noise generated by guided acoustic wave Brillouin scattering (GAWBS) is the main thermal noise in fiber channels, and its influence on quantum entanglement distribution and quantum teleportation is notable. The EPR-entangled states and the local optical fields are simultaneously transferred through an optical fiber with polarization multiplexing, which makes locking their relative phases convenient. The fidelities achieved were 0.62 and 0.69 for 6.0 and 2.0 km communication distances, which were higher than the classical teleportation and no-cloning limits, respectively [55, 68]. The extra noise during GAWBS limited the distance and fidelity of quantum teleportation, which should be reduced for longer-distance quantum teleportation. The fidelity of quantum teleportation will increase if the extra noise during GAWBS decreases.

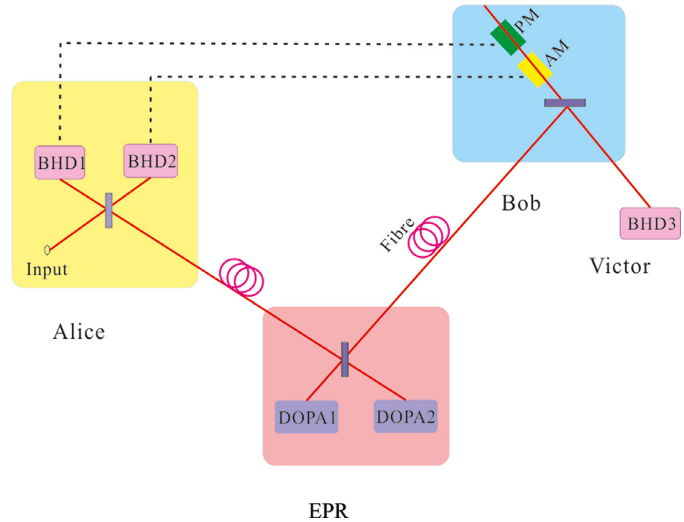

Fig. 4. A schematic of deterministic quantum teleportation through fiber channels. EPR: Einstein–Podolsky–Rosen bipartite-entangled state. DOPA: Degenerate optical parametric amplifier. PM: Phase modulator. AM: Amplitude modulator. BHD1-3: Balanced homodyne detector.

5. Conclusion and perspective

The generation and manipulation of non-classical states of light for quantum information processing and quantum measurement have achieved considerable development. Using new material and technology, the noise variance of non-classical states of light has been reduced to 10% of the vacuum noise. Thus, lower signals with less strength than the vacuum noise supported by non-classical light have been observed. CV quantum entanglement can be easily extended to multipartite entanglement due to its deterministic characteristics, which are fundamental resources for constructing multi-node quantum information networks. As practical quantum entanglement further develops, more quantum states can be unconditionally transferred in CV quantum teleportation systems to pave the way for larger-scale quantum communication and distributed quantum computation.

Declaration of Competing Interest

The authors declare that they have no conflict of interest.

Acknowledgments

The work was supported by the National Natural Science Foundation of China (Grants Nos. 61925503, 61775127, 11654002, and 11834010), the Key Project of the National Key R & D program of China (Grant No. 2016YFA0301402), the Program for the Innovative Talents of Higher Education Institutions of Shanxi, the Program for Sanjin Scholars of Shanxi Province, and the fund for Shanxi "1331 Project" Key Subjects Construction.

References

[1] J.W. Pan, Z.B. Chen, C.Y. Lu, et al., Multiphoton entanglement and interferometry, Rev. Mod. Phys. 84 (2012) 777.
[2] S.L. Braunstein, P. v. Loock, Quantum information with continuous variables, Rev. Mod. Phys. 77 (2005) 513.
[3] M.D. Reid, P.D. Drummond, W.P. Bowen, et al., Colloquium: The einstein-podolsky-rosen paradox: from concepts to applications, Rev. Mod. Phys. 81 (2009) 1727.
[4] L. Wu, H.J. Kimble, J.L. Hall, et al., Generation of squeezed states by parametric down conversion, Phys. Rev. Lett. 57 (1986) 2520.
[5] S. Shi, Y. Wang, W. Yang, et al., Detection and perfect fitting of 13.2 dB squeezed vacuum states by considering green-light-induced infrared absorption, Opt. Lett. 43 (2018) 5411.
[6] H. Vahlbruch, M. Mehmet, K. Danzmann, et al., Detection of 15 dB squeezed states of light and their application for the absolute calibration of photoelectric quantum efficiency, Phys. Rev. Lett. 117 (2016) 110801.
[7] B.J. Lawrie, P.D. Lett, A.M. Marino, et al., Quantum sensing with squeezed light, ACS Photonics 6 (2019) 1307.
[8] X. Zuo, Z. Yan, Y. Feng, et al., Quantum interferometer combining squeezing and parametric amplification, Phys. Rev. Lett. 124 (2020) 173602.
[9] J. Yu, Y. Qin, J. Qin, et al., Quantum enhanced optical phase estimation with a squeezed thermal state, Phys. Rev. Appl. 13 (2020) 024037.
[10] D. Mason, J. Chen, M. Rossi, et al., Continuous force and displacement measurement below the standard quantum limit, Nat. Phys. 15 (2019) 745.
[11] M. Tse, H. Yu, N. Kijbunchoo, et al., Quantum-enhanced advanced LIGO detectors in the era of gravitational-wave astronomy, Phys. Rev. Lett. 123 (2019) 231107.
[12] F. Acernese, Increasing the astrophysical reach of the advanced virgo detector via the application of squeezed vacuum states of light, Phys. Rev. Lett. 123 (2019) 231108.
[13] M.A. Taylor, J. Janousek, V. Daria, et al., Subdiffraction-limited quantum imaging within a living cell, Phys. Rev. X 4 (2014) 011017.
[14] W.P. Bowen, R. Schnabel, P.K. Lam, et al., Experimental characterization of continuous-variable entanglement, Phys. Rev. A 69 (2004) 012304.
[15] J. Mizuno, K. Wakui, A. Furusawa, et al., Experimental demonstration of entanglement-assisted coding using a two-mode squeezed vacuum state, Phys. Rev. A 71 (2005) 012304.
[16] T. Eberle, V. Handchen, J. Duhme, et al., Strong einstein-podolsky-rosen entanglement from a single squeezed light source, Phys. Rev. A 83 (2011) 052329.
[17] A.M. Lance, T. Symul, W.P. Bowen, et al., Tripartite quantum state sharing, Phys. Rev. Lett. 92 (2004) 177903.
[18] X. Jia, Z. Yan, Z. Duan, et al., Experimental realization of three-color entanglement at optical fiber communication and atomic storage wavelengths, Phys. Rev. Lett. 109 (2012) 253604.
[19] X. Jia, J. Zhang, Y. Wang, et al., Superactivation of multipartite unlockable bound entanglement, Phys. Rev. Lett. 108 (2012) 190501.
[20] Z. Yan, L. Wu, X. Jia, et al., Establishing and storing of deterministic quantum entanglement among three distant atomic ensembles, Nat. Commun. 8 (2017) 718.
[21] Y. Zhou, J. Yu, Z. Yan, et al., Quantum secret sharing among four players using multipartite bound entanglement of an optical field, Phys. Rev. Lett. 121 (2018) 150502.
[22] Z.Y. Ou, S.F. Pereira, H.J. Kimble, et al., Realization of the einstein-podolsky-rosen paradox for continuous variables, Phys. Rev. Lett. 68 (1992) 3663.
[23] J. Laurat, T. Coudreau, G. Keller, et al., Compact source of einstein-podolsky-rosen entanglement and squeezing at very low noise frequencies, Phys. Rev. A 70 (2004) 042315.
[24] Y. Wang, H. Shen, X. Jin, et al., Experimental generation of 6 dB continuous variable entanglement from a nondegenerate optical parametric amplifier, Opt. Express 18 (2010) 6149.
[25] C. Sayrin, I. Dotsenko, X. Zhou, et al., Real-time quantum feedback prepares and stabilizes photon number states, Nature 477 (2011) 73.
[26] R. Inoue, S.I.R. Tanaka, R. Namiki, et al., Unconditional quantum-noise suppression via measurement-based quantum feedback, Phys. Rev. Lett. 110 (2013) 163602.
[27] R.J. Nelson, Y. Weinstein, D. Cory, et al., Experimental demonstration of fully coherent quantum feedback, Phys. Rev. Lett. 85 (2000) 3045.
[28] H. Chen, J. Zhang, Phase-sensitive manipulations of the two-mode entangled state by a type-II nondegenerate optical parametric amplifier inside an optical cavity, Phys. Rev. A 79 (2009) 063826.
[29] Y. Shang, X. Jia, Y. Shen, et al., Continuous variable entanglement enhancement and manipulation by a subthreshold type II optical parametric amplifier, Opt. Lett. 35 (2010) 853.
[30] Z. Yan, X. Jia, X. Su, et al., Cascaded entanglement enhancement, Phys. Rev. A 85 (R) (2012) 040305.
[31] H.M. Wiseman, G.J. Milburn, All-optical versus electro-optical quantum-limited feedback, Phys. Rev. A 49 (1994) 4110.
[32] R. Hamerly, H. Mabuchi, Advantages of coherent feedback for cooling quantum oscillators, Phys. Rev. Lett. 109 (2012) 173602.
[33] N. Yamamoto, Coherent versus measurement feedback: Linear systems theory for quantum information, Phys. Rev. X 4 (2014) 041029.
[34] Z. Yan, X. Jia, C. Xie, et al., Coherent feedback control of multipartite quantum entanglement for optical fields, Phys. Rev. A 84 (2011) 062304.
[35] Y. Zhou, X. Jia, F. Li, et al., Quantum coherent feedback control for generation system of optical entangled state, Sci. Rep. 5 (2015) 11132.
[36] C.H. Bennett, G. Brassard, C. Crepeau, et al., Teleporting an unknown quantum state via dual classical and einstein-podolsky-rosen channels, Phys. Rev. Lett. 70 (1993) 1895.
[37] D. Bouwmeester, J.W. Pan, K. Mattle, et al., Experimental quantum teleportation, Nature 390 (1997) 575.
[38] L. Vaidman, Teleportation of quantum states, Phys. Rev. A 49 (1994) 1473.
[39] S.L. Braunstein, H.J. Kimble, Teleportation of continuous quantum variables, Phys. Rev. Lett. 80 (1998) 869.
[40] A. Furusawa, J.L. Sorensen, S.L. Braunstein, et al., Unconditional quantum teleportation, Science 282 (1998) 706.
[41] S. Pirandola, J. Eisert2, C. Weedbrook, et al., Advances in quantum teleportation, Nat. Photonics 9 (2015) 641.
[42] J.W. Pan, D. Bouwmeester, H. Weinfurter, et al., Experimental entanglement swapping: entangling photons that never interacted, Phys. Rev. Lett. 80 (1998) 3891.
[43] X. Jia, X. Su, Q. Pan, et al., Experimental demonstration of unconditional entanglement swapping for continuous variables, Phys. Rev. Lett. 93 (2004) 250503.
[44] N. Takei, H. Yonezawa, T. Aoki, et al., High-fidelity teleportation beyond the no–cloning limit and entanglement swapping for continuous variables, Phys. Rev. Lett. 94 (2005) 220502.
[45] X. Su, C. Tian, X. Deng, et al., Quantum entanglement swapping between two multipartite entangled states, Phys. Rev. Lett. 117 (2016) 240503.
[46] H. Yonezawa, T. Aoki, A. Furusawa, Demonstration of a quantum teleportation network for continuous variables, Nature 431 (2004) 430.
[47] D. Gottesman, I.L. Chuang, Demonstrating the viability of universal quantum computation using teleportation and single-qubit operations, Nature 402 (1999) 390.
[48] E. Knill, R. Laflamme, G.J. Milburn, A scheme for efficient quantum computation with linear optics, Nature 409 (2001) 46.
[49] R. Raussendorf, H.J. Briegel, A one-way quantum computer, Phys. Rev. Lett. 86 (2001) 5188.
[50] N. Lee, H. Benichi, Y. Takeno, et al., Teleportation of nonclassical wave packets of light, Science 332 (2011) 330.
[51] S. Takeda, T. Mizuta, M. Fuwa, et al., Deterministic quantum teleportation of photonic quantum bits by a hybrid technique, Nature 500 (2013) 315.
[52] J.G. Ren, P. Xu, H.L. Yong, et al., Ground-to-satellite quantum teleportation, Nature 549 (2017) 70.
[53] I. Marcikic, H. de Riedmatten, W. Tittel, et al., Long-distance teleportation of qubits at telecommunication wavelengths, Nature 421 (2003) 509.
[54] H. Takesue, S.D. Dyer, M.J. Stevens, et al., Quantum teleportation over 100 km of fiber using highly efficient superconducting nanowire single-photon detectors, Optica 2 (2015) 832.
[55] M. Huo, J. Qin, J. Cheng, et al., Deterministic quantum teleportation through fiber channels, Sci. Adv. 4 (2018) eaas9401.
[56] L.-M. Duan, G. Giedke, J.I. Cirac, et al., Inseparability criterion for continuous variable systems, Phys. Rev. Lett. 84 (2000) 2722.
[57] R. Simon, Peres-horodecki separability criterion for continuous variable systems, Phys. Rev. Lett. 84 (2000) 2726.
[58] Z.Y. Ou, S.F. Polzik, H.J. Kimble, 85% efficiency for cw frequency doubling from 1.08 to 0.54,microm, Opt. Lett. 17 (1992) 640.
[59] S. Shi, L. Tian, Y. Wang, et al., Demonstration of channel multiplexing quantum communication exploiting entangled sideband modes, Phys. Rev. Lett. 125 (2020) 070502.
[60] H. Mabuch, Coherent-feedback quantum control with a dynamic compensator, Phys. Rev. A 78 (2008) 032323.
[61] J. Kerckhoff, H.I. Nurdin, D.S. Pavlichin, et al., Designing quantum memories with embedded control: photonic circuits for autonomous quantum error correction, Phys. Rev. Lett. 105 (2010) 040502.

[62] J.E. Gough, S. Wildfeuer, Enhancement of field squeezing using coherent feedback, Phys. Rev. A 80 (2009) 042107.
[63] G.S. Agarwal, Interferences in parametric interactions driven by quantized fields, Phys. Rev. Lett. 97 (2006) 023601.
[64] J. Zhang, C. Ye, F. Gao, et al., Phase-sensitive manipulations of a squeezed vacuum field in an optical parametric amplifier inside an optical cavity, Phys. Rev. Lett. 101 (2008) 233602.
[65] Z. Yan, X. Jia, Quantum manipulation and enhancement of deterministic entanglement between atomic ensemble and light via coherent feedback control, Quantum Sci. Technol. 2 (2017) 024003.
[66] J. Yin, J. Ren, H. Lu, et al., Quantum teleportation and entanglement distribution over 100-kilometre free-space channels, Nature 488 (2012) 185.
[67] X. Ma, T. Herbst, T. Scheidl, et al., Quantum teleportation over 143 kilometres using active feed-forward, Nature 489 (2012) 269.
[68] S.L. Braunstein, Christopher, A. Fuchs, et al., Quantum versus classical domains for teleportation with continuous variables, Phys. Rev. A 64 (2001) 022321.
[69] F. Grosshans, P. Grangier, Quantum cloning and teleportation criteria for continuous quantum variables, Phys. Rev. A 64 (2001) 010301.
[70] S.L. Braunstein, C.A. Fuchs, H.J. Kimble, et al., Quantum versus classical domains for teleportation with continuous variables, Phys. Rev. A 64 (2001) 022321.
[71] N. Takei, T. Aoki, S. Koike, et al., Experimental demonstration of quantum teleportation of a squeezed state, Phys. Rev. A 72 (2005) 042304.
[72] M. Huo, J. Qin, Z. Yan, et al., Generation of two types of nonclassical optical states using an optical parametric oscillator with a PPKTP crystal, Appl. Phys. Lett. 109 (2016) 221101.

Zhihui Yan received his B.S. degree (2006) and Ph.D . degree (2012) from Shanxi University, China. He has worked in Prof. Kunchi Peng's group at the Institute of Opto-electronics, Shanxi University since 2012. He has been working as a professor at Shanxi University since 2018. His research interests focus on the fields of the quantum optics and quantum information.

Xiaojun Jia received his B. S. degree (2000) and Ph.D. (2005) degree at the Institute of Opto-Electronics from Shanxi University, China. Then he joined Prof. Kunchi Peng's group at Shanxi University. He has been working as a professor at Shanxi University since 2012. His research interests mainly focus on quantum information and quantum measurement.